Materials Science Forum Vol. 805 (2015) pp 319-324 *Online: 2014-09-12*
© (2015) Trans Tech Publications, Switzerland
doi:10.4028/www.scientific.net/MSF.805.319

Thermal Properties of a Barium Boron Silicate Glass as a Sealant for Use in Anode-Supported Solid Oxide Fuel Cells

Maviael Jose Silva[1, a], Signo Tadeu dos Reis[2,b]
and Sonia R. H. de Mello-Castanho[3,c]

[1] Nuclear and Energy Research Institute, IPEN–CNEN/SP, Brazil

[2] Missouri University of Science and Technology- Rolla MO, USA

[3] Nuclear and Energy Research Institute, IPEN–CNEN/SP, Brazil

[a]maviael.jose@usp.br(corresponding author), [b]reis@mst.edu, [c]srmello@ipen.br

Keywords: SOFC, Sealants, Glass stability, thermo-analysis, Tafel extrapolation.

Abstract. The Solid oxide fuel cell is a very efficient and clean source of energy. The planar design of SOFC requires sealant at the edges of the cell to prevent fuel leakage (H_2, CH_4, etc) and air mixing at its working temperature (700 to 900°C). The extreme operation conditions of current cell designs involve both high temperatures and highly corrosive environments. As a consequence is necessary a material to seal the chambers of the anode and cathode along each cell unit (the anode-cathode-electrolyte and interconnects). The present work is an attempt to engineering glass compositions based on the BaO-Al_2O_3-SiO_2-B_2O_3 system chosen due its thermal properties and good glass forming tendency. The glass formation or stability against crystallization and the coefficient of thermal expansion were determined by Differential Scanning Calorimeter and Dilatometric analysis, including sinterization curves. The main subject of this work is the development and selection of sealing glasses composition for SOFCs applications and also the development of new methodologies for preparation and evaluation of glass ceramics suitable for SOFC seals applications.

Introduction

In planar SOFC, fuel gas and air must kept apart from each other to avoid three main critical situations. Firstly damages in terms of efficiency to produce energy, secondly avoid aside reactions among cell components and last but not least local overheating [1,2,3]. The sealants for SOFC's must meet the following demands: should have a CET that matches in an acceptable level that of the other fuel cells components, must exhibit no adverse reactions with the joining components, and the sealant must have high chemical stability in reducing and oxidizing atmospheres[3]. It is well known that the chemical composition plays an important role in the corrosion behavior of glasses [3].However, how the amorphous structure affects the corrosion behavior of glasses is a long-term puzzling problem. It is recognized that unlike crystal alloys, glasses present unique structural characteristics without long-range periodic lattice. This structural variation in atom scale could theoretically induce even larger changes in their electrochemical properties. Nevertheless many studies have been directed only toward thermal properties in detrimental of the electrochemical properties [3,4,5]. Therefore in order to develop a suitable glass-ceramic sealant, it is necessary to understand the chemical interaction and corrosion behavior of the sealant under severe service environment, both oxidizing and reducing. This work presents the thermal and corrosion behavior of the studied sealants.

Experimental

Chemical compositions of the glass are listed in Table 1. Reagent grade BaOH, H_3BO_3, SiO_2 and Al_2O_3 > 99 wt% purity were chosen as the starting materials. After mixing the batches were melted at 1500º C for 1.5 h. The molten glass was annealed at 550º C for 1 h before cooling down to ambient temperature. The bulk glasses were milled into powder (45-50μm) for the IR, DSC, and CTE tests. The infrared spectra of the glasses were recorded at room temperature using the KBr disc

technique. A Thermo Nicolet Nexus 870 FTIR spectrometer was used to obtain the spectra in the wave number range between 400 and 2000 cm-1 with a resolution of 2 cm^{-1}. Characteristic temperatures (glass transition temperature Tg, onset and maximum crystallization temperature T_{x1} and T_{x2}, melting temperature T_m) were determined by differential scanning calorimetry (DSC) using a SETARAM MHTC 96 calorimeter at a heating rate of 10 ºC/min. The Coefficient of Thermal Expansion (CTE) of the glasses was measured using a LINSEIS L75VD1750C dilatometer with a heating rate of 5ºC/ min. The samples were analyzed by X-ray diffraction (XRD) with monochromatic CuKα radiation (λ = 0.1542 nm) using a RIGAKU DMAX 2000 PC equipment. All electrochemical measurements were conducted using a AUTOLAB PGSTAT 30 Electrochemical Measurement System. Potentiodynamic polarisation curves were measured with a potential sweep rate of 50 mV_{ref} /s in 3.0 M NaOH and HCL 2.0 M(not shown) aqueous solution after immersing the bars samples (area=10cm2) for about 30 min, when the open-circuit potential reached a steady state. All the potentials mentioned in this work were all referred to Ag/AgCl (saturated). Each electrochemical measurement was tested at least three times for repeatability. Only typical curves from an average of all measurements are presented in results. All the samples were characterized by Scaning electron microscopy SEM (Hitachi TM 3000) after polishment. The barium-boron aluminosilicate system BAS(BaO-Al_2O_3–SiO_2) with addition of B_2O_3, was chosen as the starting point for glass composition development because of its potential for good glass-forming properties.

Tabela 1 Batch compositions

Glass ID	Chemical Composition (wt %)			
	Al_2O_3	BaO	B_2O_3	SiO_2
BAS-2	4.5	77	7	11.5
BAS-4	3	74	4	19

Results and discussion.

Fig. 1 shows the infrared absorption spectra (FT-IR) of the BaO– Al_2O_3–B_2O_3–SiO_2 glassy samples BAS-0 and BAS-4. The band at about 471 cm^{-1} is due to Si–O–Si asymmetric bending vibration and the small shoulder located at 724 cm^{-1} is attributed to bending vibration of B–O–B in [BO3] triangles [4]. The main intense band located at 850–1100 cm^{-1} represents a superposition of two bands situated close to each other at about 925 and 1012 cm^{-1}, the absorption peak near 925 cm^{-1} is assigned to the stretching vibration of [BO_4] tetrahedral and the band near 1012 cm^{-1} is due to the combined stretching vibrations of Si–O–Si and B–O–B network of tetrahedral structural units [7,8]. The shoulder at 1320 cm^{-1} is due to the stretching vibration of the boroxol ring and the band centered at 1402 cm^{-1} is attributed to the B–O stretching vibration of [BO_3] triangles, characteristic for the [BO_3] group [4,5]. Even though the relationship between the CET and the concentrations of various units has not been established yet, it is possible to support the existence of boroxol groups and the maximum in CET values, based on to the observation of the band at 1320 cm^{-1} in the FT-IR spectra of the glass BAS-4[4,5,11].

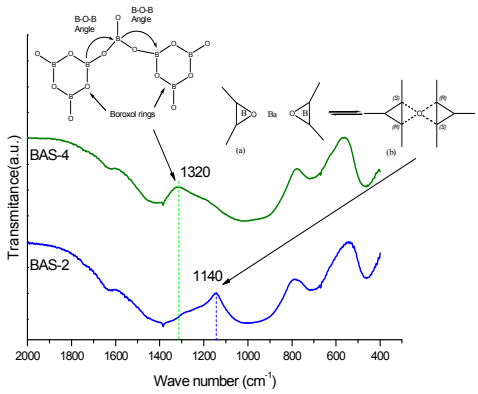

Fig. 1 FT-IR of the glass samples BAS-2 and BAS-4

Glass thermal stability. Fig. 2 shows the DSC curves of glass samples. Glasses BAS-2 and BAS-4 show two exothermic peaks, the exothermic peak of BAS-2 being very weak. The characteristic temperatures and glass stability parameters are listed in Table 2. It can be seen that an increase of Al_2O_3 (5 mol%) leads to a decrease of Tg and an increase of ΔT_x. This suggests that the introduction of Al_2O_3 to the glass system helps to improve glass stability and to decrease the trend to crystallization. A parameter usually employed to estimate the glass stability is the thermal stability, which is defined by

$$\Delta T_x = T_x - T_g \quad (1)$$

an increasing ΔT_x [3,5,8], indicates glass stability and a lower tendency toward crystallization. The CTE values of glasses are also listed in Table 2.

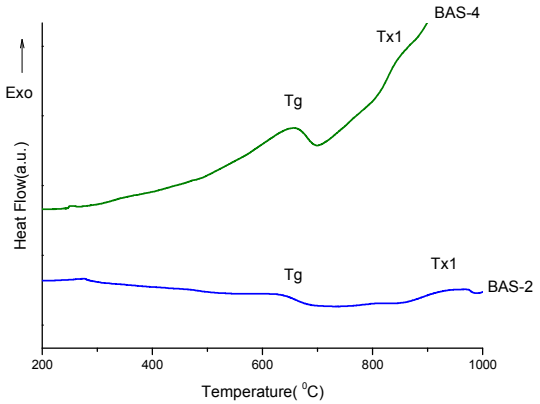

Fig. 2 DSC curves of glass samples at heating rate of 10º C/min

The CTE of the glasses are in the range 5.4 and 9.7 ppm/ºC for BAS-2 and BAS4, respectively. Thus only the sample BAS-4 can match with other components of SOFC [10,11].

Tabela 2 Summary of the thermal properties of glasses. T_g=glass transition temperature, T_{x1}=onset of maximum crystalization (T_{x2} the second one), T_m=melting temperature

Glass ID	Tg(ºC)	T_x	T_{x2}	T_{m1}	T_{m2}	ΔT_x	CET(20 to 700ºC) x 10^{-6} °C
BAS-2	488	593	766	992	-	105	5.4
BAS-4	630	819	916	-	-	189	9.7

Sintering curve results. Fig. 3 shows the linear shrinkage rate ($(dL/L_o)/dT$) as a function of temperature for the sample labeled BAS-4, the flow and shrink behavior during sintering are depicted. Shrinkage starts at about 700°C and it starts to accelerate at temperature above 750°C. Maximum shrinkage was obtained at 865.8°C for respective heating rate of 10°C/min. The joining properties for a properly sealant also depend on the flowing and wetting behavior of the glasses. Thus this temperature is a good indication for a suitable sealing temperature.

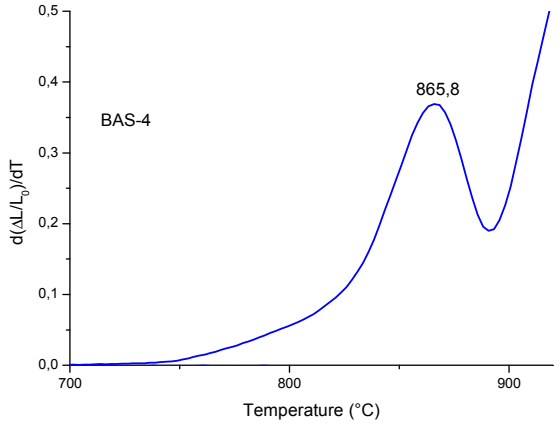

Fig. 3 Results for Linear shrinkage rate as a function of temperature

X-ray diffraction. The XRD patterns of the as-prepared BAS- glasses (not shown) depicted the appearance of a broad halo at the angle of $2\theta \approx 30^{o}$ and the absence of any diffraction peaks associated with crystalline phases indicate that the amorphous structure was formed in the annealed glasses.

Glass microstructure. As shown in Figure 4, a SEM picture of the BAS-4 sample, the scanning electron microscopy(SEM) demonstrates droplet-shaped immiscibility regions evolved in a homogeneous matrix as a result of a simple primary process[10,11]. The process of phase separation lead to the formation of halos around microphase droplets. Halos, in this case SiO_2, around droplet-shaped strongly affects the chemical properties of a glass[11].

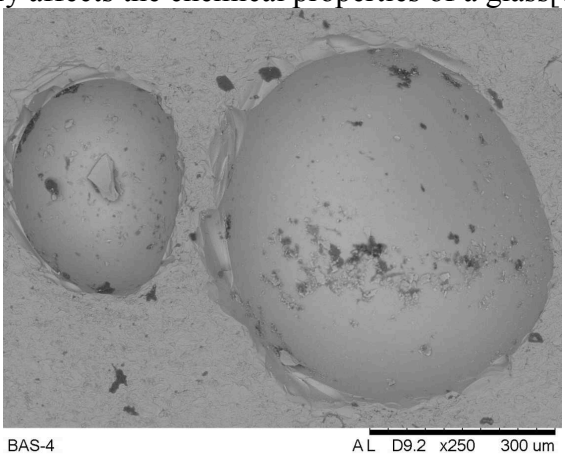

Fig. 4 SEM image of the sample BAS-2

Potentiodynamic polarization. Fig. 5 shows the potentiodynamic polarization curves for the BAS-2 and BAS-4 samples in 3.0 M NaOH aqueous solution. The corrosion current densities (i_{Corr}) were derived using Tafel extrapolation method by linear fitting of strong polarized zone (i.e. the potential is above ±100 mV_{ref} from the open-circuit potential) [9]. The corrosion current densities calculated from Tafel extrapolation method are in the order of 10^{-7} A/cm^2. All samples are passivated spontaneously with a passive current density in the order of 10^{-6} A/cm^2. Some important electrochemical parameters (including anodic and cathodic Tafel slopes, βa and βc) attained from the potentiodynamic polarization curves are summarized in Table 3.

As can be seen from the polarization curves, there is slights differences in the polarization behaviour for the BAS-4 and its counterpart, the sample BAS-2. However, the sample BAS-4 exhibits the most negative corrosion potential (E_{Corr}), and the maximum corrosion current density. Consequently, the BAS-4 sample holds the highest dissolution trend and the lowest corrosion resistance compared with the BAS-2 sample.

Tabela 3 Electrochemical parameters of each sample obtained from potentiodynamic polarization curves

Glass	$E_{Corr}(mV_{ref})$	$i_{Corr}(A/cm^2)$	βa (V_{ref})/dec	βc (V_{ref})/dec
BAS-2	-339	$6,67x10^{-7}$	3,235	2,533
BAS-4	-550	$7,701x10^{-6}$	2,308	1,88

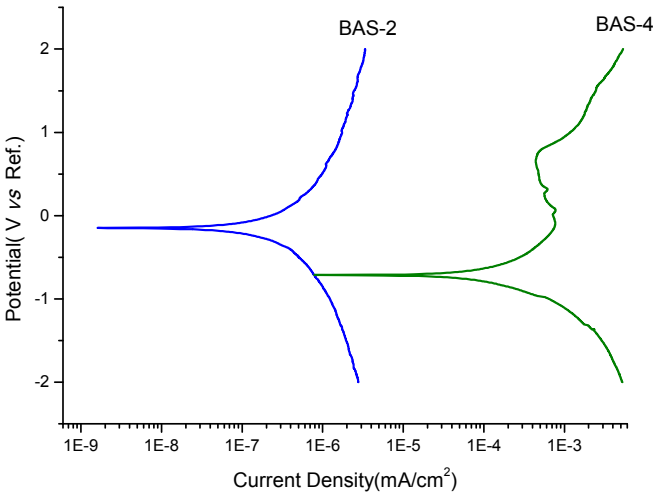

Fig, 5 Potentiodynamic polarisation curves of the glasses, BAS-2 and BAS-4 measured with a potential sweep rate of 50m V_{ref}/s in 3.0 M NaOH aqueous solution

The cathodic shift observed for the BAS-4 sample with 19 %(wt) of SiO_2 indicates that the incorporation of silica alters the cathodic kinetics on the sample surface. It is also observed that the polarization curves of the sample BAS-4 have regions of activation/passivation behavior due probably to the formation of a thin layer composed by Al_2O_3. Consequently, the sample labeled BAS-4 holds the highest dissolution trend and the lowest corrosion resistance compared with the sample, which is in according with SEM observation [5,7,9].

Conclusion.

Two glasses were prepared based on the $BaO–Al_2O_3–SiO_2$ system with the addition of B_2O_3 by the melting–annealing method in an effort to develop a suitable sealant for planar SOFC. The effects of Al_2O_3 on the glass structure were investigated. The introduction of Al_2O_3 caused the conversion of $[BO_3]$ units and $[BO_4]$ units to each other. The chemical composition plays an important role in the corrosion behavior of glasses. The sample BAS-4 comparable to the other components of SOFC it is suitable for seal.

Acknowledgments

The authors would like to thank CNPq, FAPESP, and USP for supporting this work.

References

[1] E.I. Wright, S. Rahimifard and A.J. Clegg: Journal of Power Sources Vol. 190 (2) (2009), p.362.
[2] A. Theerapapvisetpong, S. Jiemsirilers, P.Thavorniti and R. Conradt:Materials Science Forum Vol. 695 (2011), p. 1.
[3] J.W. Fergus: Journal of Power Sources Vol. 147 (1-2) (2005), p. 46.

[4] F.H. Elbatal, M.M. Khalil, N. Nada and S. Desouky: Materials Chemistry and Physics Vol. 82 (2) (2003), p. 375.
[5] M.K. Mahapatra, K. Lu: Journal of Power Sources Vol. 195 (21) (2010), p. 7129.
[6] S.E. Lin, Y.R. Cheng and W.C.J. Wei: Journal of Non-Crystalline Solids Vol. 358 (2) (2012), p. 174.
[7] N. Laorodphan, P. Namwong, W. Thiemsorn et al.: Journal of Non-Crystalline Solids Vol. 355 (1) (2009), p. 38.
[8] S.T. Reis, M.J. Pascual, R.K. Brow, C. S. Ray and T. Zhang: Journal of Non-Crystalline Solids Vol. 356 (52-54) (2010), p. 3009.
[9] W. Vanooij, D. Zhu, M. Stacy Et Al.: Tsinghua Science & Technology Vol. 10 (6) (2005), p. 639.
[10] Y. Chou, E.C. Thomsen, J. Choi and J.W. Stevenson: Journal of Power Sources Vol. 197 (2012), p. 154.
[11] S. Wegner, L. Van Wüllen and G. Tricot: Solid State Sciences Vol. 12 (4) (2010), p. 428.

A Special Issue in Memory of Dr. Lucio Salgado
10.4028/www.scientific.net/MSF.805

Thermal Properties of a Barium Boron Silicate Glass as a Sealant for Use in Anode-Supported Solid Oxide Fuel Cells
10.4028/www.scientific.net/MSF.805.319

DOI References
[1] E.I. Wright, S. Rahimifard and A.J. Clegg: Journal of Power Sources Vol. 190 (2) (2009), p.362.
http://dx.doi.org/10.1016/j.jpowsour.2009.01.069
[2] A. Theerapapvisetpong, S. Jiemsirilers, P. Thavorniti and R. Conradt: Materials Science Forum Vol. 695 (2011), p.1.
http://dx.doi.org/10.4028/www.scientific.net/MSF.695.1
[3] J.W. Fergus: Journal of Power Sources Vol. 147 (1-2) (2005), p.46.
http://dx.doi.org/10.1016/j.jpowsour.2005.05.002
[4] F.H. Elbatal, M.M. Khalil, N. Nada and S. Desouky: Materials Chemistry and Physics Vol. 82 (2) (2003), p.375.
http://dx.doi.org/10.1016/S0254-0584(03)00270-0
[5] M.K. Mahapatra, K. Lu: Journal of Power Sources Vol. 195 (21) (2010), p.7129.
http://dx.doi.org/10.1016/j.jpowsour.2010.06.003
[6] S.E. Lin, Y.R. Cheng and W.C.J. Wei: Journal of Non-Crystalline Solids Vol. 358 (2) (2012), p.174.
http://dx.doi.org/10.1016/j.jnoncrysol.2011.09.013
[7] N. Laorodphan, P. Namwong, W. Thiemsorn et al.: Journal of Non-Crystalline Solids Vol. 355 (1) (2009), p.38.
http://dx.doi.org/10.1016/j.jnoncrysol.2008.07.044
[8] S.T. Reis, M.J. Pascual, R.K. Brow, C. S. Ray and T. Zhang: Journal of Non-Crystalline Solids Vol. 356 (52-54) (2010), p.3009.
http://dx.doi.org/10.1016/j.jnoncrysol.2010.02.028
[10] Y. Chou, E.C. Thomsen, J. Choi and J.W. Stevenson: Journal of Power Sources Vol. 197 (2012), p.154.
http://dx.doi.org/10.1016/j.jpowsour.2011.09.027
[11] S. Wegner, L. Van Wüllen and G. Tricot: Solid State Sciences Vol. 12 (4) (2010), p.428.
http://dx.doi.org/10.1016/j.solidstatesciences.2009.03.021